

We are IntechOpen, the world's leading publisher of Open Access books Built by scientists, for scientists

6,900

Open access books available

186,000

International authors and editors

200M

Downloads

Our authors are among the

154

Countries delivered to

TOP 1%

most cited scientists

12.2%

Contributors from top 500 universities



WEB OF SCIENCE™

Selection of our books indexed in the Book Citation Index
in Web of Science™ Core Collection (BKCI)

Interested in publishing with us?
Contact book.department@intechopen.com

Numbers displayed above are based on latest data collected.
For more information visit www.intechopen.com



Normal Mode Analysis: A Tool for Better Understanding Protein Flexibility and Dynamics with Application to Homology Models

Jacob A. Bauer and Vladena Bauerová-Hlinková

Abstract

Molecular dynamics (MD) and normal mode analysis (NMA) are very useful methods for characterizing various dynamic aspects of biological macromolecules. In comparison to MD, NMA is computationally less expensive which facilitates the quick and systematic investigation of protein flexibility and dynamics even for large proteins and protein complexes, whose structure was obtained experimentally or *in silico*. In particular, NMA can be used to describe the flexible states adopted by a protein around an equilibrium position. These states have been repeatedly shown to have biological relevance and functional significance. This chapter briefly characterizes NMA and describes the elastic network model, a schematic model of protein shape used to decrease the computational cost of this method. Finally, we will describe the applications of this technique to several large proteins and their complexes as well as its use in enhancing protein homology modeling.

Keywords: normal mode analysis, elastic network model, crystal structure, protein dynamics, homology modeling

1. Introduction

Often there is a high demand for the structures of biologically important proteins, especially those which are large or part of complex systems. However, it is not always possible, for many reasons, to get a high-resolution structure experimentally using X-ray crystallography, NMR, or cryo-electron microscopy. Among the many problems, we can mention low protein expression, low protein stability, high aggregation or poorly diffracting crystals [1]. In this situation, *in silico* models provide a good starting point for experimental research. One of the common techniques for obtaining a reasonable structural model of a protein is homology modeling (HM). Homology modeling techniques are predominantly used to construct a hypothetical structure of a protein of interest (the target) where only the amino-acid sequence is available using the known structural features or 3D structure of one or several homologous proteins (the templates) [2–4]. However, building a static model often does not answer all questions regarding the function of the protein and its role in the cell and organism, nor does it clarify its relationship with other cellular components nucleic acids, proteins, ions and other molecules. It is important to

understand protein dynamics and flexibility, as proteins during the fulfillment of their role in the cell often change their shape, oligomeric state or even fold. As it is often very challenging to observe protein dynamics *in vivo* or *in vitro*, to understand better all these changes, a useful computational method normal mode analysis (NMA) can be used [5–9].

2. Normal mode analysis

Normal mode analysis is a technique, based on the physics of small oscillations, that can be used to describe the flexible states accessible to a protein around an equilibrium position. The idea is that when an oscillating system at equilibrium, for example a protein in an energy minimum conformation, is slightly perturbed, a restoring force acts to bring the perturbed system back to its equilibrium conformation. A system is defined to be in equilibrium or at the bottom of a potential minimum when the generalized forces acting on it are equal to zero. At the minimum energy conformation, represented by the generalized coordinates q^0 , the potential energy equation can be written as a power series in q :

$$V(q) = V(q^0) + \left(\frac{\partial V}{\partial q_i}\right)^0 \eta_i + \frac{1}{2} \left(\frac{\partial^2 V}{\partial q_i \partial q_j}\right)^0 \eta_i \eta_j + \dots \quad (1)$$

where q_i and q_j are the instantaneous configuration of components i and j and the deviation of component i from its equilibrium configuration is given by $\eta_i = q_i - q_i^0$. $V(q)$ is the potential energy equation of the system and, for proteins, usually takes the form of one of the commonly used molecular dynamics force fields [10]. The first term in the series represents the minimum value of the potential and may be set to zero and the second term will be zero at any local minimum, so the potential can be written as

$$V(q) = \frac{1}{2} \left(\frac{\partial^2 V}{\partial q_i \partial q_j}\right)^0 \eta_i \eta_j = \frac{1}{2} \eta_i V_{ij} \eta_j \quad (2)$$

where V_{ij} is the Hessian matrix which contains the second derivatives of the potential with respect to the components of the system.

It is also necessary to consider the kinetic energy (T) of the system since we are interested in dynamics. For component i , this can be given by

$$T(q) = \frac{1}{2} M \frac{d^2 \eta_i}{dt^2} \quad (3)$$

where M is a diagonal matrix containing the mass of each particle. The entire equation of motion can be written as

$$\frac{1}{2} M \frac{d^2 \eta_i}{dt^2} + \frac{1}{2} \eta_i V_{ij} \eta_j = 0 \quad (4)$$

One solution of this equation is the oscillatory equation

$$\eta_i = a_{ik} \cos(\omega_k t + \delta_k) \quad (5)$$

where a_{ik} is the amplitude of oscillation, ω_k is the frequency, and δ_k is a phase factor. By substituting this into Eq. (4), the equation of motion can be rewritten as

$$VA = \lambda A \quad (6)$$

where the matrix A contains the A_k eigenvectors of the Hessian matrix V and λ is a diagonal matrix containing the λ_k eigenvalues. The A_k eigenvectors are the normal mode vectors and describe in which direction and how far each particle in the system moves with respect to each other particle; the λ_k eigenvalues give the squares of the frequencies with which all the particles involved with a particular mode vibrate. While the eigenvectors can tell in which direction and how far each particle moves with respect to the others, it does not give absolute displacements. NMA alone therefore cannot normally be used to get the displacement amplitudes of a given normal mode [11].

The vibrational energy of the system is generally equally divided so that every vibrational mode has the same energy and the average oscillation amplitude of a given mode scales as the inverse of its frequency. Thus, modes with higher frequencies, which will have energetically greater displacements, typically describe rapid but small amplitude local motions involving relatively few atoms, while those with lower frequencies will describe slower displacements involving larger numbers of atoms and describe large-scale conformational changes. As the name of the method indicates, these vibrational modes are normal to one another, meaning that they move independently: the excitation of one mode does not trigger the motion of a second one and the general motion of the system can be described by a superposition of all the modes. These normal modes yield analytical solutions to the equations of motion: for a given set of initial positions and velocities, NMA allows us to calculate where each atom of the system in question will be at any subsequent time subject to the small oscillation approximation. (A more complete treatment of the theory behind NMA and its advantages and limitations may be found in [12]).

NMA was first applied to peptides in 1979 [13] and was subsequently used to study the whole proteins bovine pancreatic trypsin inhibitor (BPTI) [14, 15], hexokinase [16], crambin [17], human lysozyme [17, 18], ribonuclease [17], and myoglobin [19, 20]. Application of the method to larger systems was hampered by its computational expense. With advances in computer technology and the development of more efficient algorithms, it has become possible to examine larger structures, including the skeletal ryanodine receptor [21], Ca-ATPase [22], GroEL [23–25], the ribosome [26–28], the yeast nuclear pore complex [29], and virus capsids [30–32]. All these will be examined in more detail in Section 3 below.

2.1 The elastic network model

NMA is less computationally expensive than molecular dynamics simulation, but it is still not trivial for proteins containing many thousands of atoms. The first problem is that the structure to be studied must be energy minimized to ensure that the starting conformation is in a true minimum relative to the chosen force field. The minimization must then proceed until machine precision is reached, typically below 0.001 kJ/mol-nm, which is much more computationally demanding than the minimizations normally employed for other tasks. Frequently, the results of this process distort the structure, leading to NMA being carried out on a structure different from the experimentally determined one. The second problem, and the computationally limiting factor, is the diagonalization of the Hessian matrix. For classical, all-atom NMA, all N atoms in a structure, including the hydrogen atoms, must be used, making the total Hessian $3N \times 3N$ in size. For large proteins with

thousands of atoms this can become computationally difficult very quickly. Consequently, a number of coarse-grained approximate methods have been developed to overcome both of these limitations [6, 11]. The most common and widely used of these is the elastic network model (ENM).

The general idea of ENMs, first put forward by Tirion in 1996 [33], is to replace the complicated semi-empirical force fields used in standard NMA with a simple harmonic potential:

$$V(q) = \sum_{d_{ij} < R_c} C \left(d_{ij} - d_{ij}^0 \right)^2 \quad (7)$$

where d_{ij} is the distance between atoms or nodes i and j , d_{ij}^0 is the distance in the initial structure, and C is a spring constant assumed to be the same for each i - j pair. It should be noted that by design the input configuration is assumed to be a minimum energy one, and energy minimization against a potential is therefore unnecessary. R_c in this equation refers to a cut-off radius and the sum is only over all pairs less than this value. R_c is somewhat arbitrary, but in practice, values of between 7.0–8.0 Å are used based on the observed distances between non-bonded atoms in experimental structures [34, 35]. Most frequently, only the C_α atoms are used for these calculations because they are sufficient for studying the backbone motions of the protein and are all that is necessary for characterizing the lowest-frequency normal modes.

A number of different ENM formulations have been developed. The simplest one is the Gaussian network model (GNM) developed by Bahar and co-workers [36]. The GNM replaces the $3N \times 3N$ Hessian matrix with an $N \times N$ Kirchhoff matrix (Γ). Γ is defined in terms of spring constants γ_{ij} , which are created based on the assumption that the separation distance $|R_i - R_j| = R_{ij}$ between the i th and j th C_α atoms in the protein follows a Gaussian distribution. The potential is given by

$$V_{GNM} = \frac{1}{2} \sum_{ij} \gamma_{ij} \left(\Delta \overleftarrow{R}_{ij} \right)^2 \quad (8)$$

where $\Delta \overleftarrow{R}_{ij}$ is a vector expressing the fluctuations in distance between the i th and j th C_α atoms. The model assumes that these fluctuations are isotropic; consequently, no information about the three-dimensional directions of motion can be obtained. Eigenvalue decomposition of Γ does allow the contribution of individual modes to the equilibrium dynamics to be calculated, as well as the relative displacement of residues along each mode axis, the cross-correlation between the residues in the individual modes, and square displacement profiles.

Some form of the anisotropic network model (ANM) is perhaps the most commonly encountered ENM. This is the form originally suggested by Tirion [33] and incorporated into the Molecular Modeling Toolkit (MMTK) by Hinsen [37], and widely used in a number of other tools. The ANM gives the same information as the GNM, but also provides information on the directionality of the fluctuations. On the other hand, the mean-square fluctuations (B -factors) and cross-correlations it produces do not agree quite as well with experiment as GNM [38, 39]. In compensation, ANMs can be used to generate alternative conformations in the close neighborhood of the starting structure by deforming the structure along the lowest frequency modes [9]. Two groups led by Zheng [35] and Lin and Song [40] developed models which combined the best features of GNM and ANM into a single method.

While coarse-graining does allow ENMs to be scaled to very large models, it does so by losing detailed information on local structural movements. The rotating-

translating blocks (RTB) model of Sanejouand [41] was constructed to alleviate this. In this approach, the protein or other macromolecule is divided into n_β blocks made up of one or a few residues connected by elastic springs. Next, it is assumed that a good approximation to the low-frequency normal modes can be made by forming linear combinations of the local rotations and translations of these individual blocks. Consequently, a $3N \times 6n_\beta$ projection matrix P is constructed and used to build a projected Hessian matrix H_β , which is diagonalized with $A_\beta^T H_\beta A_\beta = \Lambda_\beta$, where A_β is the eigenvector matrix diagonalizing H_β and Λ_β is the corresponding eigenvalue matrix. The resulting eigenvectors can be projected back into the full $3N$ -dimensional space using $A_P = PA_\beta$, where A_P is a $3N \times 6n_\beta$ matrix containing the $6n_\beta$ lowest-frequency approximate normal modes.

3. Applications

In a survey of the recent structural biology literature, Bauer *et al.* [12] found that NMA, as a component of a structural study, most often was used for describing the overall flexible motions of a molecule or for determining how those motions might be correlated with ligand binding or catalytic activation. Another use for NMA is to study the motions of macromolecules or macromolecular assemblies that are too large for treatment using conventional MD simulation. It has been shown that the low-frequency normal modes and the first few principal components calculated from a MD simulation overlap considerably, meaning that NMA can plausibly substitute for MD for large systems when only the overall collective motions of the system are needed [42–44]. Below, we will examine the application of NMA to experimentally obtained protein structures as well as to protein HM studies.

3.1 Application to experimental structures

3.1.1 Ryanodine receptor

The ryanodine receptors (RyRs) are the largest presently known ion channels, with molecular weights of 2.2 MDa. They are homotetramers embedded in the membrane of the sarcoplasmic reticulum of myocytes, where they play a key role in excitation-contraction coupling. They regulate Ca^{2+} release from the sarcoplasmic reticulum by undergoing a closed-to-open gating transition in response to an action potential or calcium binding. RyRs are found in all animals. Three isoforms have been identified in mammals: RyR1 (predominantly expressed in skeletal muscle), RyR2 (cardiac muscle) and RyR3 (present in several tissues including the brain, diaphragm, and testes) [45–47]. RyR malfunction leads to severe muscular disorders, including malignant hyperthermia, central core disease, tachycardia, dysplasia, and others [45]. The first high-resolution cryo-EM structures of the complete rabbit skeletal RyR were reported in 2015 [48–50], and were followed by a number of other high-resolution structures of the skeletal and cardiac isoforms in both their open and closed conformations, either alone or bound to regulators (For review see Bauerová-Hlinková *et al.* [51]).

A number of MD simulation studies have been reported for both the skeletal and cardiac RyR isoforms, but only covering small parts of the whole channel; in particular, the N-terminal domain (roughly the first 600 amino acids) [52–55] and parts of the channel domain [56–58] were studied in this way. Generally, these studies focused on identifying how known disease-causing mutations affected the dynamics of these fragments.

Shortly after the appearance of the first high-resolution cryo-EM structures, Wenjun Zheng published a normal-mode analysis on the 3.8-Å RyR1 structure [21]. He found that the largest collective motions of the closed form involved large outward and downward movements of the peripheral domains, in good agreement with the conformational variations observed in multiple cryo-EM structures of the closed form later reported by des Georges *et al.* [59]. By using normal mode analysis to flexibly fit the closed form into a 10 Å cryo-EM map of the open form, he was also able to create a model of the open form of the receptor. A similar open-form conformation was created by Mowrey *et al.* [56] using an ion-pulling molecular dynamics simulation on only the transmembrane portion of the structure. Both models recreated the major features of the RyR1 and RyR2 open-channel structures reported subsequently, including the rotation of an important pore-lining transmembrane α -helix away from the channel axis.

3.1.2 Ca^{2+} -ATPase

The Ca^{2+} -ATPase may be thought of as the partner of the RyR. While RyR releases Ca^{2+} from the sarcoplasmic reticulum into the cytosol, the Ca^{2+} -ATPase pumps it back in, against a large concentration gradient, at the rate of two Ca^{2+} ions per hydrolyzed ATP. Conventionally, the Ca^{2+} -ATPase is thought to take two different states: E1, which has high affinity for Ca^{2+} , and E2, which has much lower affinity [60, 61]. In addition to the binding and dissociation of Ca^{2+} , ATP hydrolysis and dephosphorylation of the resulting phosphorylated Asp351 result in the presence of 4–7 different physiological states [62]. At least 54 crystal structures have been determined since the first one in 2000 [63] and they cover nearly all the conformations of the different physiological states. They show large conformational rearrangements during the reaction cycle and have been investigated by a number of computational methods [62]. Most of the NMA studies occurred soon after the initial structures by Toyoshima *et al.* [63, 64] had been reported, but before the final ones had become available [65, 66], making this a good situation for illustrating both the abilities and limitations of NMA.

The initial structure [63] showed that the ATPase consisted of three cytoplasmic domains, labeled A (activation), N (nucleotide binding), and P (phosphorylation), and 10 transmembrane helices (M1–M10). As the names suggest, the cytoplasmic domain N holds most of the ATP binding site and P holds the phosphorylation site. Subsequent structures [65, 66] showed that the A domain also participates in ATP binding and has a crucial role in dephosphorylation. In the first structure, taken to be in the E1 conformation, the N and A domains were widely separated. Subsequent E2 structures showed that ATP binding induces a large movement in the N domain and a smaller, though still considerable, motion in the A domain. NMA on only the initial E1 structure [67] found that the N domain seemed to be the most mobile and that rotational hinges were present between the N and P, and A and M domains. It was also suggested that the transmembrane α -helices M2, M4, and M8 likely played an important role in Ca^{2+} release into the sarcoplasmic reticulum lumen. After the second structure in the E2 conformation became available [64], two studies examined the normal modes that participate in the E1 \rightarrow E2 conformational change [22, 68]. They found that only a few of the lower-frequency modes were needed to describe the E1 \rightarrow E2 transition, which predominantly involved the movement of the A and N domains to close the cytoplasmic headpiece. They also both predicted that the transmembrane domain was likely to undergo a twisting motion which would eliminate the Ca^{2+} binding sites and open up the channel. The results of these studies were partially confirmed by the subsequent structures [65, 66]. The first

NMA study [67] did correctly predict that the largest conformational changes would be observed in the positions of the N and A domains, and the movement of helices M2, M4, and M8 was important for Ca^{2+} release, but they all missed that transmembrane helix M5 underwent a sharp bend following ADP release. They also failed to note that a conserved loop from domain A which interacts with the phosphate binding site shifts conformation and plays an important role in hydrolyzing the phosphate free from Asp351. Thus, these coarse-grained NMA studies managed to successfully predict many of the large-scale movements, but missed an important local conformational change and a large distortion of an element of secondary structure.

3.1.3 GroEL

Escherichia coli GroEL is one of the best studied chaperones and it is essential for cell viability [69, 70]. It is composed of two identical rings of seven subunits each. Each 548-residue subunit can be further subdivided into apical, intermediate, and equatorial domains, and the two rings stack back-to-back to form an isolated chamber where a non-native substrate can be refolded. The three domains are separated by upper and lower hinges, making each subunit highly flexible. GroEL works together with the co-chaperone GroES, which also has seven subunits and can bind to the apical part of either GroEL ring to form a cap [71]. During its activity cycle, GroEL goes through a number of conformational changes which are triggered by ATP binding and hydrolysis, interactions with GroES, and the substrate protein. When bound to no ligands, GroEL is in what is termed the “tense” or T state; this state is the most attractive to a (partially) unfolded substrate. Binding of ATP shifts GroEL to the “relaxed” or R state, and GroES binding and subsequent ATP hydrolysis shift it to the R' state.

The structural transitions between these forms have been well described [70–75], and NMA has been applied to study the dynamics of both the individual subunits as well as the entire GroEL–GroES complex [5, 23–25, 76–78]. The earliest studies [23, 24] examined individual GroEL subunits and found that there is a very close relationship between their flexibility and the conformational changes observed for the entire complex. When ATP binds to a given subunit, the subunit changes conformation closely following a few low-frequency normal modes [23].

NMA was also calculated on an ENM of the whole GroEL–GroES complex [25]. These authors found that the slowest normal modes revealed a wide variety of motions which depended on the central cavity of the structure. These included the opposite twisting of the two GroEL rings combined with a flattening and expansion of the GroES cap; bending, shear, opposed radial breathing of the two rings, and stretching and contraction along the complex's long axis were also observed. They concluded that the mechanical motions driven by the different modes provide changing binding surfaces and differently sized cavities in the interior which might enable differently shaped substrates to be accommodated; possibly, these shifts might also be used during the refolding process.

3.1.4 The Ribosome

The ribosome is a molecular machine for translating the nucleotide sequence encoded in an mRNA transcript into a polypeptide sequence that folds into a functional protein. In prokaryotes, it is composed of a 50S subunit (containing a 23S rRNA, a 5S rRNA, and 34 proteins) and a 30S subunit (comprised of a 16S rRNA and 21 proteins) which together combine to form a 70S ribosome. The 30S subunit

binds the mRNA and the anticodon end of the bound tRNA and is responsible for mRNA decoding. The 50S subunit interacts with the ends of the tRNA bound to the transferred amino acid and catalyzes peptide bond formation. The complete assembly features three sites for tRNA placement: an A (aminoacyl) site, a P (peptidyl) site, and an E (exit) site.

Several different crystal structures of ribosomes from different organisms and in different states have been determined by both X-ray crystallography and cryo-EM. The earliest were the 30S subunit from *Thermus thermophilus* at 3.0 Å [79, 80] and 3.3 Å resolution [81], the 50S subunit from *Haloarcula marismortui* at 2.4 Å [82, 83], and the complete *T. thermophilus* 70S ribosome at 5.5 Å [84]. These structures were the ones most commonly used for NMA studies. Many of these studies were carried out in the laboratory of Robert Jernigan [27, 85–89]. Overall, they found that the dominant motion was a ratchet motion between the large and small subunits, which was very similar to that observed experimentally by cryo-EM [26, 88]. This motion is observed regardless of whether the tRNAs and mRNA are present [87]. Curiously enough, this motion also remains even if all the proteins are stripped out, provided the general shape is maintained [27, 87]. This suggests that the motion arises from the ribosome structure itself and is not dependent upon the presence of its substrates.

Many other complex motions have been observed, especially at the mRNA decoding center in the 30S subunit [87]. In particular, the mRNA A site was found to be more flexible than the P site, which was consistent with the experimentally observed *B*-factors. It also agrees with the observation that the A site is able to accommodate a diverse set of substrates and that the P site needs to be more rigid to ensure the fidelity of the codon–anticodon matching. The collective dynamics of the exit tunnel for the growing polypeptide was also examined [28]. Here, it was found that the tunnel could be generally divided into three regions, entrance, neck, and exit, based on the low-frequency motions of the tunnel lining. Generally, the middle parts of the tunnel move in a complex way toward the tunnel exit, while the parts near the exit itself rotate around the tunnel axis. NMA of ENMs of the tRNAs were also examined and shown to be similar to the range of conformations observed from multiple experimental tRNA structures [89]. By comparing the normal modes of tRNAs alone and bound to the ribosome, they also noted that the ribosome acts to suppress all internal tRNA motions, only allowing it to move by rigid-body translation [90].

3.1.5 Yeast nuclear pore complex

The nuclear pore complex (NPC) is an enormous macroassembly that regulates the import and export of a large variety of substances (including proteins, nucleic acids, and small molecules) from the nucleus [91]. It is an octagonal complex composed of some 30 different proteins called nucleoporins. The yeast NPC has a mass of around 60 MDa while the vertebrate one is around 125 MDa. The yeast NPC is a ring that is around 100 nm across with a central pore of about 30 nm. The eight different subunits are termed “spokes” and each spoke exhibits pseudo 2-fold symmetry, giving the complex as a whole pseudo 16-fold symmetry. With 16 copies each, the 30 different nucleoporins make a total complex of 450–480 proteins. The central channel is coated with several “FG nucleoporins,” which contain many structurally disordered phenylalanine (F) and glycine (G) repeats. These FG nucleoporins form a selective barrier: small particles (< 30 kDa) can diffuse freely through the pore, while larger proteins require the assistance of karyopherin transport factors. The vertebrate NPC possesses, in addition to a central core, additional structural elements, including a cytoplasmic ring, a nuclear ring, and a luminal ring [91].

By following an integrative approach that combined data from many different sources, a coarse-grained structural model of the yeast NPC was developed [92, 93].

This model was then used for a coarse-grained NMA using an ENM [29]. This study found that two types of collective modes were predicted to be favored: a global bending mode and an extension and contraction mode that oscillated between a circle and an ellipse. Several different coarse-grained representations were tried and it was found that a simple model of a toroid with an axial varying mass density was sufficient to capture the main dynamic features. It was also found that the number of spokes significantly affected the number of symmetric low-frequency modes: toroids composed of eight spokes had access to symmetric modes that toroids composed of seven or nine spokes did not. A similar NMA study created using a different coarse-grained toroidal model came to similar conclusions [94].

3.1.6 Virus Capsids

Aside from the ryanodine receptor and the nuclear pore complex, all of the forgoing examples are molecular machines of some sort that transform the chemical energy of ATP hydrolysis into mechanical motion. Viral capsids are different in that they are more of an architectural than a mechanical structure. Viral capsids encapsulate and protect the viral genome during its spread from cell to cell during infection. They can display a number of different surface features, including pores, canyons, spikes, and pillars. They typically consist of more than 100 protein subunits and have diameters of 100 nm or more. Capsids with more than 60 subunits that maintain their icosahedral symmetry are typically made up of collections of pentamers and hexamers [95]. The most commonly studied viral capsids form a spherical or icosahedral shape. NMA has been used to study the mechanical properties and conformational changes of these capsids for nearly 20 years (reviewed by May [96]). Even using coarse-grained NMA methods, the computational loads required to study whole capsids are still non-trivial, so a variety of symmetry-based approaches have been created to reduce them [32, 97–103].

One of the most thoroughly studied viral capsids is that of bacteriophage HK97 [31, 99, 104]. Tama and Brooks [31, 105] used NMA to study the swelling of a number of viral capsids, including cowpea chlorotic mottle virus (CCMV), Nudaurelia capensis virus (N ω V), and HK97. They found that for CCMV and N ω V, only the single lowest-frequency mode was needed to describe the swelling, while HK97 required the two lowest-frequency modes. The reason for this appeared to be that the CCMV and N ω V, being spherical, required only a single mode, while HK97 not only expands, but also changes conformation from spherical to icosahedral. Generally, these studies, together with two others [106, 107], showed that the functional dynamics of the capsids are dictated by their structure, which is why only the lowest-frequency modes are needed. The HK97 expansion and conformational transition occurs during its maturation, and NMA has also been applied to study the HK97 maturation pathway [99, 104]. During maturation, a spherical procapsid undergoes substantial expansion together with a conformational change from spherical to icosahedral to form a mature capsid. These studies found that only a few low-frequency icosahedral modes were needed to account for most of the maturation expansion and that maturation appears to occur through the puckering of the pentamers followed by the flattening and cross-linking of the hexamers.

3.2 NMA in homology modeling studies

3.2.1 Membrane proteins

One of the protein groups in which homology modeling has been used together with NMA is multidomain transmembrane proteins, in particular the human

nicotine acetylcholine receptor (hnAChR) [108] and *E. coli* mechanosensitive channel (MscL) [109]. hnAChRs are located mainly in the central nervous system and mediate fast neurotransmission. They possess a homopentameric quaternary structure where each monomer consists of an extracellular domain involving a conserved Cys loop and a ligand-binding channel, four transmembrane domains, and an intracellular segment. MscL is an integral membrane protein that gates in response to membrane tension in order to diminish the turgor pressure when bacteria are moved from a high to a low osmolarity environment. Like nAChR, MscL is a homopentamer where each subunit is composed of a cytoplasmic and a transmembrane domain.

Similar approaches were used in both studies. First a homology model of the target protein was constructed based on the known structures of similar proteins, followed by the application of NMA. The aim of both studies was to better understand channel gating and the particular structural changes associated with it [108, 109]. The hnAChR study also involved predicting the ligand binding site [108].

3.2.2 Enzymes

Enzymes have also been studied using a combination of HM and NMA. One example is the *Arabidopsis thaliana* Dicer-like 4 protein (AtDCL4) [110]. Dicer-like 4 is a large multidomain protein belonging to the Ribonuclease III family and is involved in the regulation of gene expression and antiviral defense through RNA-interference pathways. In particular, AtDCL4 produces short-stranded RNAs (ta-siRNA) which are incorporated into the RNA-induced silencing complex to direct the silencing of cognate RNA [111, 112]. The main aim of the study [110] was to better understand the mechanism of AtDCL4-mediated dsRNA recognition and binding by which small RNAs of a specific size are produced. First, the authors built the core of the AtDCL4 protein, which consists of a Platform, a PAZ domain, a Connector helix and RNaseA/B domains. A model of an AtDCL4–dsRNA complex was then constructed, which suggested that the spatial orientation of the AtDCL4 domains with respect to one another are responsible for the length of the bound dsRNA. Two regions, one on the surface of the Platform domain and second in the PAZ loop, were also identified, which are likely to be responsible for RNA binding.

3.2.3 Cell division and transport proteins

One of the longest-studied cellular processes is cell division [113] and cellular transport [114]. Regarding cell division, a combination of HM and NMA was used to study a yeast cohesin, an essential ring-shaped chromosome maintenance protein that mediates sister chromatid cohesion, homologous recombination, and DNA looping. This protein is a member of the structural maintenance of chromosomes (Smc) family, which exists in all eukaryotes [115]. In yeast, cohesin mainly consists of two Smc proteins, Smc1 and Smc3, both of which adopt long, anti-parallel coiled-coil regions that are separated by two globular regions: an ATP-binding head domain and a hinge region. The aim of the HM and NMA study [113] was to reveal the missing molecular details of how the two halves of the hinge region open to create an entry gate for DNA. In agreement with experimental data, the constructed yeast cohesin HM model showed that the bending motion of the cohesin ring is able to adopt a head-to-tail conformation. At the interface of the cohesin heterodimer, low-frequency conformational changes were observed to deform the highly conserved glycine residues present there. Normal mode analysis further revealed that the docking of large globular structures, such as the nucleosome and accessory proteins, to cohesin notably affected the mobility of the coiled-coil regions. Moreover, fully

solvated molecular dynamics calculations, performed specifically on the hinge region, indicated that hinge opening starts from one side of the dimerization interface and is coordinated by the highly conserved glycine residues [113].

4. Conclusions

Normal mode analysis is a very useful technique for determining which conformational states are accessible to a given macromolecule. It can provide much of the same information given by more computationally expensive methods, such as molecular dynamics simulation, at only a fraction of the cost. It can be used by itself or in tandem with HM to characterize the general flexibility and domain movements of a molecule, to produce possible alternative conformations and confirm observed ones, and to describe the conformational changes that occur or might occur during substrate binding, product release, or catalytic activation. We have illustrated its utility using several examples of its application to a number of large biologically important proteins and protein complexes from bacteria, eukaryotes, and viruses. The biological relevance of the *in silico* models constructed by HM and NMA can be verified and expanded by different experimental approaches involving molecular and structural biology and biochemistry.

Acknowledgements

The authors would like to thank Eva Kutejová for general support during the writing of this chapter.

This research was funded by Vedecká Grantová Agentúra MŠVVaŠ SR and SAV grant number 2/0131/20.

Conflict of interest


The authors declare no conflict of interest.

Author details

Jacob A. Bauer* and Vladena Bauerová-Hlinková
Institute of Molecular Biology, Slovak Academy of Sciences, Bratislava, Slovakia

*Address all correspondence to: jacob.bauer@savba.sk

IntechOpen

© 2020 The Author(s). Licensee IntechOpen. This chapter is distributed under the terms of the Creative Commons Attribution License (<http://creativecommons.org/licenses/by/3.0>), which permits unrestricted use, distribution, and reproduction in any medium, provided the original work is properly cited. 

References

- [1] McPherson A. Crystallization of Biological Macromolecules. Cold Spring Harbor, NY: Cold Spring Harbor Laboratory Press; 1999.
- [2] Xiang Z. Advances in homology protein structure modeling. *Curr Protein Pept Sci*. 2006;7:217–227.
- [3] Lohning AE, Levonis SM, Williams-Noonan B, Schweiker SS. A Practical Guide to Molecular Docking and Homology Modeling for Medicinal Chemists. *Curr Top Med Chem*. 2017;17: 2023–2040.
- [4] Muhammed MT, Aki-Yalcin E. Homology modeling in drug discovery: Overview, current applications, and future perspectives. *Chem Biol Drug Des*. 2019;93:12–20.
- [5] Ma J. Usefulness and Limitations of Normal Mode Analysis in Modeling Dynamics of Biomolecular Complexes. *Structure*. 2005;13:373–380.
- [6] Skjaerven L, Hollup SM, Reuter N. Normal mode analysis for proteins. *J Mol Struct Theochem*. 2009;898:42–48.
- [7] López-Blanco JR, Chacón P. New generation of elastic network models. *Curr Opin Struct Biol*. 2016;37:46–53.
- [8] Tiwari SP, Reuter N. Conservation of intrinsic dynamics in proteins — what have computational models taught us? *Curr Opin Struct Biol*. 2018;50:75–81.
- [9] Bahar I, Lezon TR, Bakan A, Shrivastava IH. Normal Mode Analysis of Biomolecular Structures: Functional Mechanisms of Membrane Proteins. *Chem Rev*. 2010;110:1463–1497.
- [10] González MA. Force fields and molecular dynamics simulations. *Collection SFN*. 2011;12:169–200.
- [11] Mahajan S, Sanejouand YH. On the relationship between low-frequency normal modes and the large-scale conformational changes of proteins. *Arch Biochem Biophys*. 2015;567:59–65.
- [12] Bauer JA, Pavlovič J, Bauerová-Hlinková V. Normal Mode Analysis as a Routine Part of a Structural Investigation. *Molecules*. 2019;24:3293.
- [13] Levy RM, Karplus M. Vibrational Approach to the Dynamics of an α -helix. *Biopolymers*. 1979;18:2465–2495.
- [14] Noguti T, Gō N. Collective variable description of small-amplitude conformational fluctuations in a globular protein. *Nature*. 1982;296:776–778.
- [15] Brooks B, Karplus M. Harmonic dynamics of proteins: Normal modes and fluctuations in bovine pancreatic trypsin inhibitor. *Proc Natl Acad Sci USA*. 1983;80:6571–6575.
- [16] Harrison RW. Vibrational Calculation of the Normal Modes of a Large Macromolecule: Methods and some Initial Results. *Biopolymers*. 1984; 23:2943–2949.
- [17] Levitt M, Sander C, Stern PS. Protein Normal-mode Dynamics: Trypsin Inhibitor, Crambin, Ribonuclease and Lysozyme. *J Mol Biol*. 1985;181:423–447.
- [18] Brooks B, Karplus M. Normal modes for specific motions of macromolecules: Application to the hinge-bending mode of lysozyme. *Proc Natl Acad Sci USA*. 1985;82:4995–4999.
- [19] Seno Y, Gō N. Deoxymyoglobin Studied by the Conformational Normal Mode Analysis I. Dynamics of Globin and the Heme–Globin Interaction. *J Mol Biol*. 1990;216:95–109.
- [20] Seno Y, Gō N. Deoxymyoglobin Studied by the Conformational Normal

Mode Analysis II. The Conformational Change upon Oxygenation. *J Mol Biol.* 1990;216:111–126.

[21] Zheng W. Toward decrypting the allosteric mechanism of the ryanodine receptor based on coarse-grained structural and dynamic modeling. *Proteins.* 2015;83:2307–2318.

[22] Li G, Cui Q. Analysis of Functional Motions in Brownian Molecular Machines with an Efficient Block Normal Mode Approach: Myosin-II and Ca^{2+} -ATPase. *Biophys J.* 2004;86:743–763.

[23] Ma J, Karplus M. The allosteric mechanism of the chaperonin GroEL: A dynamic analysis. *Proc Natl Acad Sci USA.* 1998;95:8502–8507.

[24] Ma J, Sigler PB, Xu Z, Karplus M. A Dynamic Model for the Allosteric Mechanism of GroEL. *J Mol Biol.* 2000;302:303–313.

[25] Keskin O, Bahar I, Flatow D, Covell DG, Jernigan RL. Molecular Mechanisms of Chaperonin GroEL–GroES Function. *Biochemistry.* 2002;41:491–501.

[26] Tama F, Valle M, Frank J, Brooks III CL. Dynamic reorganization of the functionally active ribosome explored by normal mode analysis and cryo-electron microscopy. *Proc Natl Acad Sci USA.* 2003;100:9319–9323.

[27] Yan A, Wang Y, Klockowski A, Jernigan RL. Effects of Protein Subunits Removal on the Computed Motions of Partial 30S Structures of the Ribosome. *J Chem Theory Comput.* 2008;4:1757–1767.

[28] Kurkcuoglu O, Kurkcuoglu Z, Doruker P, Jernigan RL. Collective dynamics of the ribosomal tunnel revealed by elastic network modeling. *Proteins.* 2009;75:837–845.

[29] Lezon TR, Sali A, Bahar I. Global Motions of the Nuclear Pore Complex:

Insights from Elastic Network Models. *PLoS Comput Biol.* 2009;5:e1000496.

[30] Lee BH, Jo S, Choi Mk, Kim MH, Choi JB, Kim MK. Normal mode analysis of Zika virus. *Comput Biol Chem.* 2018;72:53–61.

[31] Tama F, Brooks III CL. Diversity and Identity of Mechanical Properties of Icosahedral Viral Capsids Studied with Elastic Network Normal Mode Analysis. *J Mol Biol.* 2005;345:299–314.

[32] van Vlijmen HWT, Karplus M. Normal Mode Calculations of Icosahedral Viruses with Full Dihedral Flexibility by Use of Molecular Symmetry. *J Mol Biol.* 2005;350:528–542.

[33] Tirion MM. Large Amplitude Elastic Motions in Proteins from a Single-Parameter, Atomic Analysis. *Phys Rev. Lett.* 1996;77:1905–1908.

[34] Miyazawa S, Jernigan RL. Estimation of Effective Interresidue Contact Energies from Protein Crystal Structures: Quasi-Chemical Approximation. *Macromolecules.* 1985;18:534–552.

[35] Zheng W. A Unification of the Elastic Network Model and the Gaussian Network Model for Optimal Description of Protein Conformational Motions and Fluctuations. *Biophys J.* 2008;94:3853–3857.

[36] Bahar I, Atilgan AR, Erman B. Direct evaluation of thermal fluctuations in proteins using a single-parameter harmonic potential. *Folding Des.* 1997;2:173–181.

[37] Hinsen K. The Molecular Modeling Toolkit: A New Approach to Molecular Simulations. *J Comp Chem.* 2000;21:79–85.

[38] Bahar I, Rader AJ. Coarse-grained normal mode analysis in structural biology. *Curr Opin Struct Biol.* 2005;15:586–592.

- [39] Cui Q, Bahar I, editors. Normal Mode Analysis. Theory and Applications to Biological and Chemical Systems. Boca Raton, Florida, USA: Chapman & Hall/CRC; 2006.
- [40] Lin TL, Song G. Generalized spring tensor models for protein fluctuation dynamics and conformation changes. *BMC Struct Biol.* 2010;10(Suppl 1):S3.
- [41] Durand P, Trinquier G, Sanejouand YH. A New Approach for Determining Low-Frequency Normal Modes in Macromolecules. *Biopolymers.* 1994;34:759–771.
- [42] Rueda M, Chacón P, Orozco M. Thorough Validation of Protein Normal Mode Analysis: A Comparative Study with Essential Dynamics. *Structure.* 2007;15:565–575.
- [43] Rueda M, Ferrer-Costa C, Meyer T, Pérez A, Camps J, Hospital A, et al. A consensus view of protein dynamics. *Proc Natl Acad Sci USA.* 2007;104:796–801.
- [44] Doruker P, Atilgan R Ali, Bahar I. Dynamics of Proteins Predicted by Molecular Dynamics Simulations and Analytical Approaches: Application to α -Amylase Inhibitor. *Proteins.* 2000;40: 512–524.
- [45] Lanner JT, Georgiou DK, Joshi AD, Hamilton SL. Ryanodine Receptors: Structure, Expression, Molecular Details, and Function in Calcium Release. *Cold Spring Harb Perspect Biol.* 2010;2:a003996.
- [46] Van Petegem F. Ryanodine Receptors: Structure and Function. *J Biol Chem.* 2012;287:31624–31,632.
- [47] Van Petegem F. Ryanodine Receptors: Allosteric Ion Channel Giants. *J Mol Biol.* 2015;427:31–53.
- [48] Zalk R, Clarke OB, des Georges A, Grassucci RA, Reiken S, Mancina F, et al. Structure of a mammalian ryanodine receptor. *Nature.* 2015;517:44–49.
- [49] Yan Z, Bai Xc, Yan C, Wu J, Li Z, Xie T, et al. Structure of the rabbit ryanodine receptor RyR1 at near-atomic resolution. *Nature.* 2015;517:50–55.
- [50] Efremov RG, Leitner A, Aebersold R, Raunser S. Architecture and Conformational Switch Mechanism of the Ryanodine Receptor. *Nature.* 2015;517:39–43.
- [51] Bauerová-Hlinková V, Hajdúchová D, Bauer JA. Structure and Function of the Human Ryanodine Receptors and Their Association with Myopathies – Present State, Challenges, and Perspectives. *Molecules.* 2020;.
- [52] Bauer JA, Borko v, Pavlović J, Kutejová E, Bauerová-Hlinková V. Disease-associated mutations alter the dynamic motion of the N-terminal domain of the human cardiac ryanodine receptor. *J Biomol Struct Dyn.* 2020;38: 1054–1070.
- [53] Yamazawa T, Ogawa H, Murayama T, Yamaguchi M, Oyamada H, Suzuki J, et al. Insights into channel modulation mechanism of RYR1 mutants using Ca^{2+} imaging and molecular dynamics. *J Gen Physiol.* 2020;152:e201812235.
- [54] Zheng W, Liu Z. Investigating the inter-subunit/subdomain interactions and motions relevant to disease mutations in the N-terminal domain of ryanodine receptors by molecular dynamics simulation. *Proteins.* 2017;85: 1633–1644.
- [55] Xiong J, Liu X, Gong Y, Zhang P, Qiang S, Zhao Q, et al. Pathogenic mechanism of a catecholaminergic polymorphic ventricular tachycardia causing-mutation in cardiac calcium release channel RyR2. *J Mol Cell Cardiol.* 2018;117:26–35.
- [56] Mowrey DD, Xu L, Mei Y, Pasek DA, Meissner G, et al. Ion-pulling simulations provide insights into the

mechanisms of channel opening of the skeletal muscle ryanodine receptor. *J Biol Chem.* 2017;292:12947–12,958.

[57] Schilling R, Fink RHA, Fischer WB. MD simulations of the central pore of ryanodine receptors and sequence comparison with 2B protein from coxsackie virus. *Biochim Biophys Acta.* 2014;1838:1122–1131.

[58] Schilling R, Fink RHA, Fischer WB. Interaction of ions with the luminal sides of wild-type and mutated skeletal muscle ryanodine receptors. *J Mol Model.* 2016;22:37.

[59] des Georges A, Clarke OB, Zalk R, Yuan Q, Condon KJ, Grassucci RA, et al. Structural basis for gating and activation of RyR1. *Cell.* 2016;167:145–157.

[60] Albers RW. Biochemical aspects of active transport. *Annu Rev. Biochem.* 1967;36:727–756.

[61] Post RL, Hegyvary C, Kume S. Activation by Adenosine Triphosphate in the Phosphorylation Kinetics of Sodium and Potassium Ion Transport Adenosine Triphosphatase. *J Biol Chem.* 1972;247:6530–6540.

[62] Kobayashi C, Koike R, Ota M, Sugita Y. Hierarchical domain-motion analysis of conformational changes in sarcoplasmic reticulum Ca^{2+} -ATPase. *Proteins.* 2015;83:746–756.

[63] Toyoshima C, Nakasako M, Nomura H, Ogawa H. Crystal structure of the calcium pump of sarcoplasmic reticulum at 2.6 Å resolution. *Nature.* 2000;405:647–655.

[64] Toyoshima C, Nomura H. Structural changes in the calcium pump accompanying the dissociation of calcium. *Nature.* 2002;418:605–611.

[65] Toyoshima C, Mizutani T. Crystal structure of the calcium pump with a

bound ATP analogue. *Nature.* 2004;430:529–535.

[66] Toyoshima C, Nomura H, Tsuda T. Luminal gating mechanism revealed in calcium pump crystal structures with phosphate analogues. *Nature.* 2004;432:361–368.

[67] Li G, Cui Q. A Coarse-Grained Normal Mode Approach for Macromolecules: An Efficient Implementation and Application to Ca^{2+} -ATPase. *Biophys J.* 2002;83:2457–2474.

[68] Reuter N, Hinsén K, Lacap'ère JJ. Transconformations of the SERCA1 Ca-ATPase: A Normal Mode Study. *Biophys J.* 2003;85:2186–2197.

[69] Thirumalai D, Lorimer GH. Chaperonin-Mediated Protein Folding. *Annu Rev. Biophys Biomol Struct.* 2001;30:245–269.

[70] Horwich AL. Chaperonin-Mediated Protein Folding. *J Biol Chem.* 2013;288:23622–23,632.

[71] Xu Z, Horwich AL, Sigler PB. The crystal structure of the asymmetric GroEL–GroES–(ADP)₇ chaperonin complex. *Nature.* 1997;388:741–750.

[72] Chaudhry C, Horwich AL, Brunger AT, Adams PD. Exploring the Structural Dynamics of the *E. coli* Chaperonin GroEL Using Translation-libration-screw Crystallographic Refinement of Intermediate States. *J Mol Biol.* 2004;342:229–245.

[73] Hyeon C, Lorimer GH, Thirumalai D. Dynamics of allosteric transitions in GroEL. *Proc Natl Acad Sci USA.* 2006;103:18939–18,944.

[74] Liu J, Sankar K, Wang Y, Jia K, Jernigan RL. Directional Force Originating from ATP Hydrolysis Drives the GroEL Conformational Change. *Biophys J.* 2017;112:1561–1570.

- [75] de Groot BL, Vriend G, Berendsen HJC. Conformational Changes in the Chaperonin GroEL: New Insights Into the Allosteric Mechanism. *J Mol Biol.* 1999;286:1241–1249.
- [76] Yang Z, Májek P, Bahar I. Allosteric Transitions of Supramolecular Systems Explored by Network Models: Application to Chaperonin GroEL. *PLoS Comput Biol.* 2009;5:e1000360.
- [77] Na H, Jernigan RL, Song G. Bridging between NMA and Elastic Network Models: Preserving All-Atom Accuracy in Coarse-Grained Models. *PLoS Comput Biol.* 2015;11:e1004542.
- [78] Zheng W, Brooks BR, Thirumalai D. Allosteric Transitions in the Chaperonin GroEL are Captured by a Dominant Normal Mode that is Most Robust to Sequence Variations. *Biophys J.* 2007;93: 2289–2299.
- [79] Wimberly BT, Brodersen DE, Clemons Jr. WM, Morgan-Warren RJ, Carter AP, Vonnrhein C, et al. Structure of the 30S ribosomal subunit. *Nature.* 2000;407:327–339.
- [80] Carter AP, Clemons WM, Brodersen DE, Morgan-Warren RJ, Wimberly BT, Ramakrishnan V. Functional insights from the structure of the 30S ribosomal subunit and its interactions with antibiotics. *Nature.* 2000;407:340–348.
- [81] Schlutzenzen F, Tocilj A, Zarivach R, Harms J, Gluehmann M, Janell D, et al. Structure of Functionally Activated Small Ribosomal Subunit at 3.3 Å Resolution. *Cell.* 2000;102:615–623.
- [82] Ban N, Nissen P, Hansen J, Moore PB, Steitz TA. The Complete Atomic Structure of the Large Ribosomal Subunit at 2.4 Å Resolution. *Science.* 2000;289:905–920.
- [83] Nissen P, Hansen J, Ban N, Moore PB, Steitz TA. The Structural Basis of Ribosome Activity in Peptide Bond Synthesis. *Science.* 2000;289: 920–930.
- [84] Yusupov MM, Yusupova GZ, Baucom A, Lieberman K, Earnest TN, Cate JHD, et al. Crystal Structure of the Ribosome at 5.5 Å Resolution. *Science.* 2001;292:883–896.
- [85] Zimmermann MT, Jia K, Jernigan RL. Ribosome Mechanics Informs about Mechanism. *J Mol Biol.* 2016;428:802–810.
- [86] Kurkcuoglu O, Turgut OT, Cansu S, Jernigan RL, Doruker P. Focused Functional Dynamics of Supramolecules by Use of a Mixed-Resolution Elastic Network Model. *Biophys J.* 2009;97: 1178–1187.
- [87] Kurkcuoglu O, Doruker P, Sen TZ, Kloczkowski A, Jernigan RL. The ribosome structure controls and directs mRNA entry, translocation and exit dynamics. *Phys Biol.* 2008;5:046005.
- [88] Wang Y, Rader AJ, Bahar I, Jernigan RL. Global ribosome motions revealed with elastic network model. *J Struct Biol.* 2004;147:302–314.
- [89] Zimmermann MT, Jernigan RL. Elastic network models capture the motions apparent within ensembles of RNA structures. *RNA.* 2014;20:792–804.
- [90] Wang Y, Jernigan RL. Comparison of tRNA Motions in the Free and Ribosomal Bound Structures. *Biophys J.* 2005;89:3399–3409.
- [91] Wentz SR, Rout MP. The Nuclear Pore Complex and Nuclear Transport. *Cold Spring Harb Perspect Biol.* 2010;2: a000562.
- [92] Alber F, Dokudovskaya S, Veenhoff LM, Zhang W, Kipper J, Devos D, et al. Determining the architectures of macromolecular assemblies. *Nature.* 2007;450:683–694.

- [93] Alber F, Dokudovskaya S, Veenhoff LM, Zhang W, Kipper J, Devos D, et al. The molecular architecture of the nuclear pore complex. *Nature*. 2007;450:695–701.
- [94] Wolf C, Mofrad MRK. On the Octagonal Structure of the Nuclear Pore Complex: Insights from Coarse-Grained Models. *Biophys J*. 2008;95:2073–2085.
- [95] Caspar DLD, Klug A. Physical Principles in the Construction of Regular Viruses. *Cold Spring Harb Symp Quant Biol*. 1962;27:1–24.
- [96] May ER. Recent Developments in Molecular Simulation Approaches to Study Spherical Virus Capsids. *Mol Simul*. 2014;40:878–888.
- [97] van Vlijmen HWT, Karplus M. Normal mode analysis of large systems with icosahedral symmetry: Application to (Dialanine)₆₀ in full and reduced basis set implementations. *J Chem Phys*. 2001;115:691–698.
- [98] Ming D, Kong Y, Wu Y, Ma J. Substructure synthesis method for simulating large molecular complexes. *Proc Natl Acad Sci USA*. 2003;100:104–109.
- [99] Kim MK, Jernigan RL, Chirikjian GS. An elastic network model of HK97 capsid maturation. *J Struct Biol*. 2003;143:107–117.
- [100] Dykeman EC, Sankey OF. Atomistic modeling of the low-frequency mechanical modes and Raman spectra of icosahedral virus capsids. *Phys Rev. E Stat Nonlin Soft Matter Phys*. 2010;81:021918.
- [101] Chen X, Sun Y, An X, Ming D. Virtual interface substructure synthesis method for normal mode analysis of super-large molecular complexes at atomic resolution. *J Chem Phys*. 2011;135:144108.
- [102] Lu M, Ming D, Ma J. fSUB: Normal Mode Analysis with Flexible Substructures. *J Phys Chem B*. 2012;116:8636–8645.
- [103] Martín-Bravo M, Llorente JMG, Hernández-Rojas J. A minimal coarse-grained model for the low-frequency normal mode analysis of icosahedral viral capsids. *Soft Matter*. 2020;16:3443–3455.
- [104] Rader AJ, Vlad DH, Bahar I. Maturation Dynamics of Bacteriophage HK97 Capsid. *Structure*. 2005;13:413–421.
- [105] Tama F, Brooks III CL. The Mechanism and Pathway of pH Induced Swelling in Cowpea Chlorotic Mottle Virus. *J Mol Biol*. 2002;318:733–747.
- [106] Englert F, Peeters K, Taormina A. Twenty-four near-instabilities of Caspar-Klug viruses. *Phys Rev. E Stat Nonlin Soft Matter Phys*. 2008;78:031908.
- [107] Peeters K, Taormina A. Group theory of icosahedral virus capsid vibrations: A top-down approach. *J Theor Biol*. 2009;256:607–624.
- [108] Haddadian EJ, Cheng MH, Coalson RD, Xu Y, Tang P. In Silico models for the Human $\alpha 4\beta 2$ Nicotinic Acetylcholine Receptor. *J Phys Chem B*. 2008;112:13981–13,990.
- [109] Valadié H, Lacapčre JJ, Sanejouand YH, Etchebest C. Dynamical Properties of the MscL of *Escherichia coli*: A Normal Mode Analysis. *J Mol Biol*. 2003;332:657–674.
- [110] Mickiewicz A, Sarzyńska J, Miłostan M, Kurzyńska-Kokorniak A, Rybarczyk A, Łukasiak P, et al. Modeling of the catalytic core of *Arabidopsis thaliana* Dicer-like 4 protein and its complex with double-stranded RNA. *Comput Biol Chem*. 2017;66:44–56.
- [111] Brodersen P, Sakvarelidze-Achard L, Bruun-Rasmussen M, Dunoyer P,

Yamamoto YY, Sieburth L, et al.
Widespread Translational Inhibition by
Plant miRNAs and siRNAs. *Science*.
2008;320:1185–1190.

[112] Vazquez F, Hohn T. Biogenesis and
Biological Activity of Secondary siRNAs
in Plants. *Scientifica*. 2013;2013:783253.

[113] Kurkcuoglu O, Bates PA.
Mechanism of Cohesin Loading onto
Chromosomes: A Conformational
Dynamics Study. *Biophys J*. 2010;99:
1212–1220.

[114] Serohijos AWR, Chen Y, Ding F,
Elston TC, Dokholyan NV. A structural
model reveals energy transduction in
dynein. *Proc Natl Acad Sci USA*. 2006;
103:18540–18,545.

[115] Nasmyth K, Haering CH. Cohesin:
its roles and mechanisms. *Annu Rev*.
Genet. 2009;43:525–558.